Case Report

BIOMEDICAL Journal of Scientific & Technical Research

ISSN: 2574 -1241

DOI: 10.26717/BJSTR.2023.52.008314

# Bangle Rhizome Extract Promotes Hippocampal Neurogenesis Associated with Improved Cognitive Functions: A Case Study

**Takuji Shirasawa[1,2]*, Kazumi Hirano[3], Masakazu Namihira[3], Luis Carlos Aguilar Cobos[4] and Tatefuji Tomoki[5]**

[1]*Ochanomizu Health and Longevity Clinic, Japan*

[2]*Shirasawa Anti-Aging Medical Institute, Japan*

[3]*Molecular Neurophysiology Research Group, Biomedical Research Institute, The National Institute of Advanced Industrial Science and Technology (AIST), Japan*

[4]*Livant Neurorecovery Center, Mexico*

[5]*Hosoda SHC Company Ltd., Japan*

***Corresponding author:** Takuji Shirasawa, Ochanomizu Health and Longevity Clinic, Tokyo 101-0062, Shirasawa Anti-Aging Medical Institute, Tokyo 101-0062, Japan

**ARTICLE INFO**

**Received:** September 06, 2023

**Published:** September 13, 2023

**Citation:** Takuji Shirasawa, Kazumi Hirano, Masakazu Namihira, Luis Carlos Aguilar Cobos and Tatefuji Tomoki. Bangle Rhizome Extract Promotes Hippocampal Neurogenesis Associated with Improved Cognitive Functions: A Case Study. Biomed J Sci & Tech Res 52(5)-2023. BJSTR. MS.ID.008314.

**ABSTRACT**

Bangle Rhizome Extract (BRE) promotes neurogenesis of human neural stem cells and improves spatial learning memory in ageing model mice. In the present case study, we applied BRE to a 53-year-old female patient with mild memory impairment for 6 weeks. We examined cognitive functions, P300 Electroencephalogram (EEG) signals, and MRI signals before and after the administration of BRE. Spatial memory, working memory, attention, and reaction time were improved after BRE administration in association with hippocampal neurogenesis. EEG recordings showed improved electrical abnormalities with increased neural connections and enhanced EEG responses in attention and visual spatial memory tests. MRI showed the fusion of fragmented tissues in the hippocampus after BRE administration, which represents morphological changes observed in the regenerative process of the hippocampus. This is the first clinical case report that BRE promotes neurogenesis and regeneration of the hippocampus associated with improved cognitive functions.

**Keywords:** Bangle Extract; Hippocampal Neurogenesis; Cognitive Function

**Abbreviations:** BRE: Bangle Rhizome Extract; EEG: Electroencephalogram; hfNSCs: Human Foetal Neural Stem Cells; NCI: Neurocognition Index; DG: Dentate Gyrus; SD: Standard Deviation

## Introduction

Bangle, Zingiber Purpureum Rosc., is a tropical ginger widely distributed in Southeast Asia. Bangle has been used as a traditional Indonesian medicine known as "Jamu" for the treatment of fever, headaches, stomach pain, rheumatism, obesity, postpartum problems, and COVID-19 infection [1,2]. Chemical analysis showed that Bangle Rhizome Extract (BRE) contains cis- and trans-3-(3,4-dimethoxyphenyl)-4-[(E)-3,4-dimethoxystyryl] cyclohex-1-enes (c- and t-banglenes) and dimers of (E)-1-(3,4- dimethoxyphenyl) butadiene [3,4]. These chemical compounds showed neurotrophic activity in PC12 cells and protective activity against cell death caused by deprivation of serum in primary culture of mouse cortical neurons [5]. In an animal model of nondegenerative diseases, chronic treatment with BRE in senescence-accelerated prone-8 (SAMP8) mice improved spatial learning and memory deficits with enhanced hippocampal

neurogenesis [6]. We recently showed that BRE induces the proliferation and differentiation of Human Foetal Neural Stem Cells (hfNSCs) by activating the canonical Wnt/ß-catenin signalling pathway as a mechanism of neuronal differentiation [7]. Safety assessment and oral toxicity tests of BRE have been performed [3]; however, clinical applications of BRE for patients with cognitive decline have not been published to date. In this study, we present for the first time a human case study in which BRE administration induced neurogenesis and regeneration of the hippocampus with improved cognitive functions.

## Materials and Methods

### Materials

Bangle Rhizome Extract powder (Hosoda SHC Co., Fukui, Japan) contained trans- and cis-3-(3′,4′-dimethoxyphenyl)-4-[(E)-3″,4″-dimethoxystyryl] cyclohex-1-ene (phenylbutenoid dimers; 5.0%) and was composed of 20.2% Bangle extract, 8.5% emulsifier, and 71.3% dextrin. Bangle Rhizome Extract (BRE) tablets (200 mg/tablet) containing 85 mg/tablet of BRE powder (22.7 mg/tablet of BRE containing 5 mg/tablet of c- and t-banglenes), sucrose fatty acid ester, and dextrin were made from powder, pregelatinized starch (Asahi Kasei Chemicals, Tokyo, Japan), Xantan gum (Ina Food Industry, Nagano, Japan), silicon dioxide (CDSL, Japan, Tokyo), and shellac (Gifu Shellac Manufacturing, Gifu, Japan) [3].

### Cognitive Evaluation

The Cognitrax standard package was used to examine neurocognitive functions [8]. The patient performed 10 tasks displayed on a personal computer: Verbal Memory, Visual Memory, Finger Tapping, Symbol Digit Coding, Stroop Test, Shifting Attention, Continuous Performance, Perception of Emotions, Non-Verbal Reasoning, and 4-part Continuous Performance Test. Based on the scores on the 10 tasks, a composite Neurocognition Index (NCI) and 15 domain scores (composite memory, verbal memory, visual memory, psychomotor speed, reaction time, processing speed, motor speed, composite attention, sustained attention, simple attention, cognitive flexibility, executive function, social acuity, reasoning, and working memory) were calculated. Individual scores were standardized by setting the mean score to 100 and the Standard Deviation (SD) to 15; therefore, the scores in participants can be compared to those in healthy people without investigating healthy people [8]. A higher score indicates better neurocognitive function.

### Electrophysiological Study

NuAmps EEG/ERP Amplifier (NeuroScanTM, https://compumedicsneuroscan.com/products-overview/) was used to collect EEG data across 20 channels during five paradigms:

1. A resting state paradigm in which participants sat quietly with their eyes open and then closed for 3 min each,
2. A P300 paradigm that involved an active listening task in which participants were asked to count rate deviant (1,500 Hz) tones presented amongst frequent standard (1,000 Hz) tones,
3. An attention paradigm in which participants were asked to hit the keyboard when the letter "T" appeared on the screen followed by the letter "S",
4. A visual space paradigm in which participants were asked to answer how many flashing boxes appeared on the screen, and
5. A mental flexibility paradigm in which participants were asked to determine the sorting manner of cards using the Wisconsin Card Sorting Test. Collected EEG data were analysed by NeuroScanTM Software (SCAN version 4.3, now version up to CURRY 9, https://compumedicsneuroscan.com/products-overview/) for P300 analysis, the visual spatial memory test, the attention test, the mental flexibility test, and coherence analysis.

### Cell Culture and Immunostaining

hfNSCs were purchased from Phoenix Songs Biologicals, Inc. (PSB, Branford, CT) (Cat# 23001-003, Donor Lot CxB-3). In preparation for establishing hfNSC lines, informed consent was obtained from the donor or the donor's next of kin by the PSB company (https://phoenixsongsbio.com/). The cell line was derived from the human cerebral cortex of a male foetus at embryonic week 14. Culture methods for hfNSCs have been described previously [7,9,10], and the neural aspect of this cell line was confirmed. In brief, hfNSCs were cultured in N2-supplemented Dulbecco's modified Eagle's medium with F12 (DMEM/F12, GIBCO, Waltham, MA) containing a 0.1% B27 supplement (GIBCO), 10 ng/ml human basic fibroblast growth factor (FGF; R&D Systems Inc., Minneapolis, MN), and 20 ng/ml human epidermal growth factor (EGF; PeproTech, Inc., Rocky Hill, NJ) on culture dishes that had been precoated with poly-l-ornithine (Sigma Aldrich, St. Louis, MO) and laminin (Corning, Corning, NY). A maximum of 30 cell passages were used. For neuronal differentiation, hfNSCs were placed into neurobasal medium (GIBCO) containing 2% B27 supplement (GIBCO) and 0.5 mM l-glutamine (Nacalai Tesque, Inc., Kyoto, Japan). For immunostaining, cells were washed with phosphate-buffered saline (PBS), fixed in 4% paraformaldehyde in PBS, and stained with appropriate antibodies against βIII-tubulin and β-catenin. Nuclei were stained after fixation using Hoechst 33342 (Dojindo Laboratories, Kumamoto, Japan). Stained cells were visualized with a fluorescence microscope (BX53, Olympus, Tokyo, Japan).

### Molecular Illustration

The 3D chemical structure of banglene, 1beta-(3,4-dimethoxystyryl)-2alpha-(3,4-dimethoxyphenyl)-3-cyclohexene (PubChem CID 53494256), was imported from the PubChem library (https://pubchem.ncbi.nlm.nih.gov/docs/about). The 3D protein structures of Wnt, LRP6, Frizzled, Dvl (Dishevelled), Axin, GSK 3ß, ß-catenin, LEF, and tau were retrieved from the RCSB Protein Data Bank (RCSB PDB, https://www.rcsb.org) and then imported into UCSF Chimae-

ra-X (https://www.cgl. ucsf.edu/chimaerax/). The molecules are displayed with molecular surfaces coloured by amino acid hydrophobicity or electrostaticity.

## Case Presentation

A 53-year-old Japanese woman developed gradual progression of memory impairment with well-preserved language comprehension, emotional control, and spatial and temporal orientation. Her cognitive function examination on December 9, 2022, using Cognitrax revealed mild reasoning impairment (Cognitrax score = 76), while working memory, reaction time, motor speed, cognitive flexibility, executive function, spatial memory, and attention were normal with a Cognitrax Total Score of 108.0. Blood chemistry, CBC, and HbA1c analysis failed to indicate any disorder associated with memory impairment. MRI data acquired on August 3, 2021, showed no remarkable atrophy of the cerebral cortex and no vascular pathologies, while endoscopic in silico view of hippocampi showed degeneration at the upper part of the neck in the left hippocampus (Figure 1A), indicated by red and blue arrows) and fragmentation at the head and upper part of the neck in the right hippocampus (Figure 1B), indicated by violet and yellow arrows). Electrophysiological evaluation on December 13, 2022, showed that asymmetrical P300 EEG responses were detected between the right parietal lead (P3) and left parietal lead (P4) (Figure 2A) red lines). The visual spatial memory test showed hyperexcitable EEG reactions at the left frontolateral lead (F7) and right frontolateral lead (F8), suggesting that degenerative pathology in the frontal lobe caused the memory problems (Figure 3B), red lines).

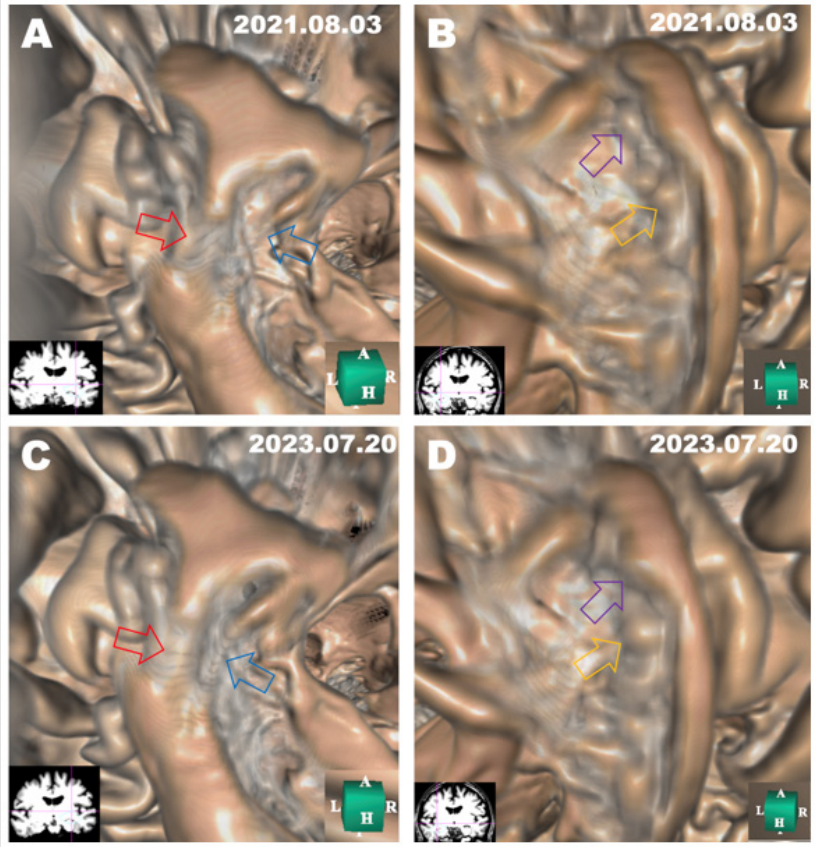


**Figure 1:** Morphological evaluation before and after Bangle extract administration. MRI scans were performed on August 3, 2021, and on July 20, 2023, before and after Bangle extract administration. Endoscopic in silico views were rendered using Expert INTAGER software from MRI T1-weighted images with 1-mm sagittal slices.
A, B: Endoscopic in silico views of the left hippocampus
A. And right hippocampus
B. Before Bangle extract administration.
C, D: Twelve weeks after Bangle extract administration, both hippocampi showed regeneration of the damaged tissues; left hippocampus.
C. And right hippocampus.
D. Coloured arrows indicate the degenerated parts of the hippocampus before (A, B) and the regenerated hippocampus after Bangle extract administration (C, D).

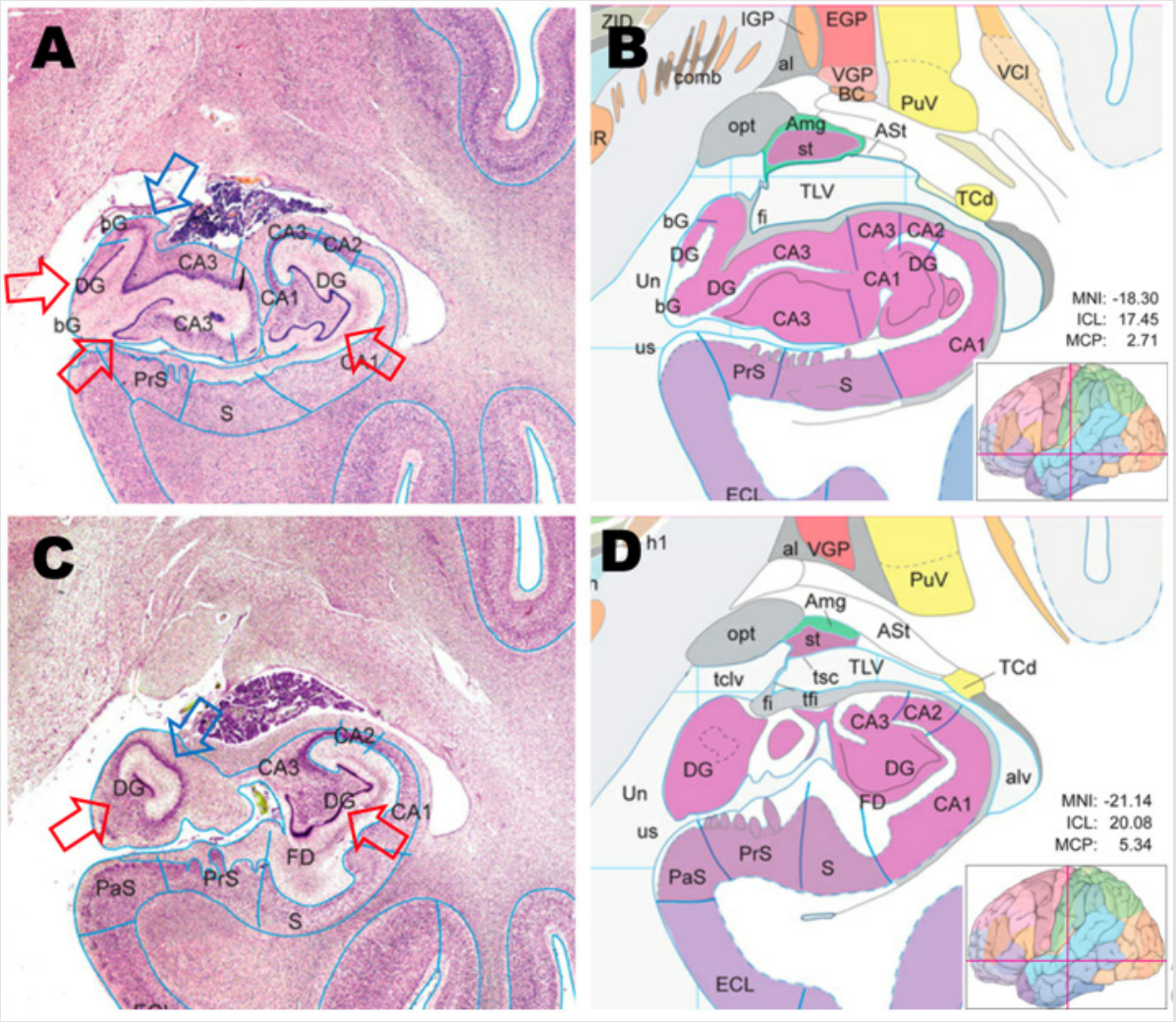


**Figure 2:** Histological atlas of the human hippocampus. The histological sections (A, C) and colour atlas (B, D) of the human hippocampus were modified from the book "ATLAS OF THE HUMAN BRAIN" (Academic Press, 2016) [20]. Coronal sections in the neck of the left hippocampus with H&E staining at 17.45 mm (A) or 20.08 mm posterior from the centre of the anterior commissure (C). The median portion of the Dentate Gyrus (DG) and the lateral portion of the DG are indicated by red arrows. CA3 layers are indicated by blue arrows. MNI (stereotactic image from MRI study), distance from centre of AC in MNI space. MCP, distance from Midcommissural Point (MCP). ICL, distance from centre of AC.

The attention test also showed hyperexcitable EEG responses in both frontopolar leads (FP1 and FP2) with symmetrical reactions with a later phase peak at 750 msec (Figure 3C). The mental flexibility test using the Wisconsin Card Sorting System showed a hyperexcitable reaction with 10,000 μV2 at 850 msec at the left frontopolar lead (FP1) (Figure 3D), implying that the generation of ideas may be mildly impaired due to degenerative pathology in the frontal lobe. Overall, the degenerative pathology in the hippocampus and frontal lobe, partly in the parietal lobe, may contribute to the symptoms of memory impairment. Coherence analysis showed a mild decrease in the number of neural connections at left frontolateral (F7), left temporal (T3 and T5), left central (C3), left occipital (O1), right frontolateral (F8), right temporal (T4 and T6), and right occipital (O2) leads (Figures 4A & 4C). We therapeutically applied 6 tablets of Bangle Rhizome Extract (BRE) every day for 12 weeks and evaluated cognitive function at 6 weeks and 12 weeks as well as electrophysiological evaluation at 12 weeks, as shown in (Figure 5). On February 3, 2023, 6 weeks after administration of BRE, cognitive function tests showed improvement in reasoning (76 -> 90) and cognitive enhancement in working memory (98 -> 118), spatial memory (90 -> 116), reaction time (102 -> 111), and attention (92 -> 107) with an improvement in Cognitrax Total Scores (108.0 -> 111.0) (Figure 5).

**DOI:** 10.26717/BJSTR.2023.52.008314

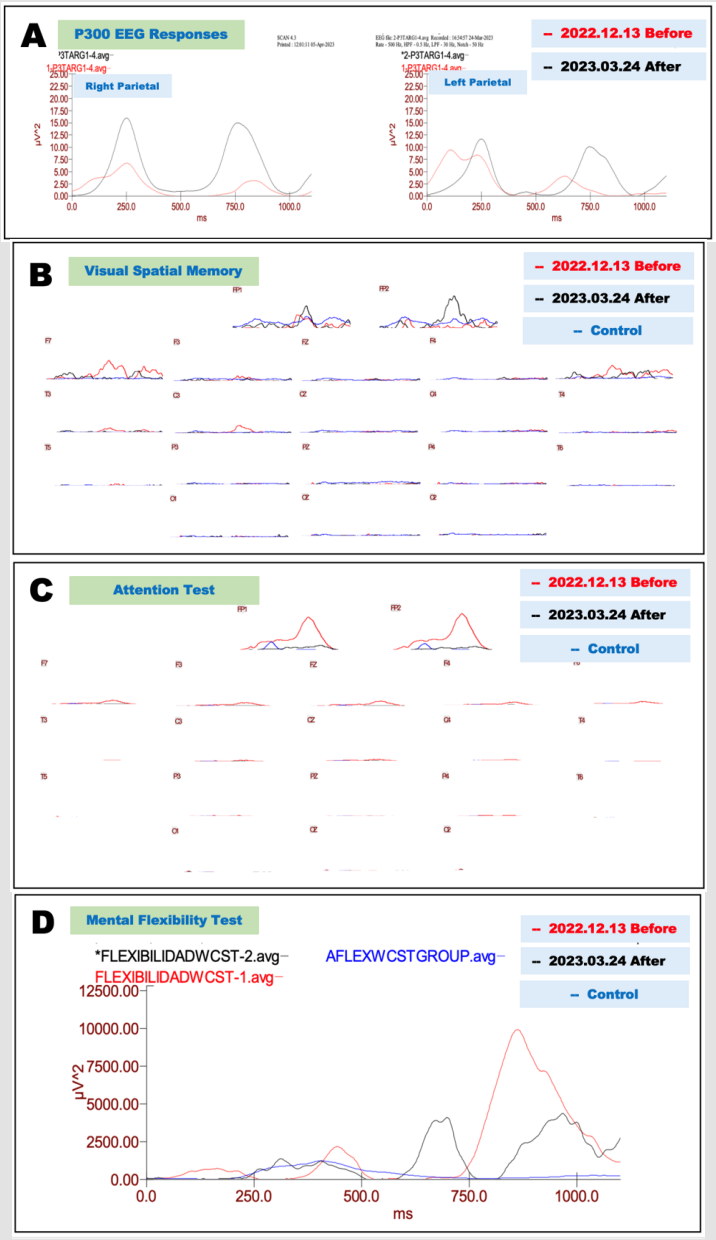


**Figure 3:**

A. Electrophysiological evaluation of P300 EEG responses before and after Bangle extract administration. Before bangle extract administration, P300 EEG responses (red lines) recorded on December 13, 2022, with high-pitched sound showed asymmetrical responses in parietal leads. After Bangle extract administration, asymmetrical P300 responses significantly improved and showed symmetrical P300 EEG recorded on March 24, 2023 (black lines).

B. Before bangle extract administration, EEG responses in the visual spatial memory test (red lines) recorded on December 13, 2022, showed hyperexcitabilities in the frontal leads (F7 and F8) and left central lead (C3). After Bangle extract administration, the hyperexcitabilities significantly improved and showed enhanced relevant responses in frontopolar leads (FP1 and FP2) recorded on March 24, 2023 (black lines) compared to control responses (blue lines).

C. Before bangle extract administration, EEG responses in the attention test (red lines) recorded on December 13, 2022, showed hyperexcitabilities in frontopolar leads (FP1 and FP2). After Bangle extract administration, the hyperexcitabilities significantly improved in frontopolar leads (FP1 and FP2) recorded on March 24, 2023 (black lines) compared to control responses (blue lines).

D. Before bangle extract administration, EEG responses in the mental flexibility test using the Wisconsin Card Sorting Test (red lines) recorded on December 13, 2022 showed hyperexcitabilities in the left frontopolar lead (FP1). After Bangle extract administration, the hyperexcitabilities significantly improved but were still higher than those of the control in the left frontopolar lead (FP1) recorded on March 24, 2023 (black lines) compared to the control responses (blue lines).

**DOI:** 10.26717/BJSTR.2023.52.008314

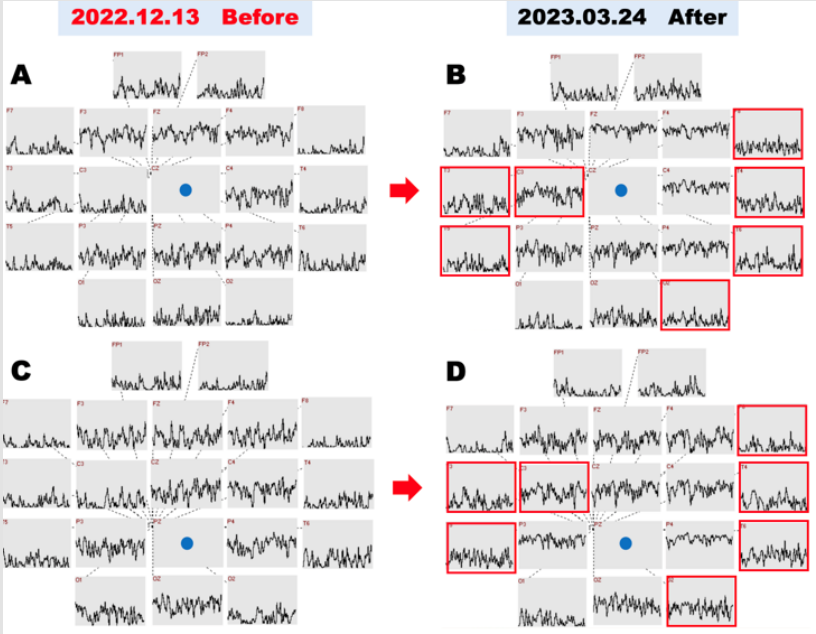


**Figure 4:** Coherence analysis before and after Bangle extract administration. Coherence analysis during P300 EEG responses showed the neuronal connections between the central lead (CZ) (blue circle) and other cortical leads (A) or between the central parietal lead (PZ) (blue circle) and other cortical leads (C) before BRE administration. The number of neural connections was increased at the left temporal (T3 and T5), left central (C3), right frontolateral (F8), right temporal (T4 and T6), and right occipital (O2) leads (Figures 4B-4D, red boxes).

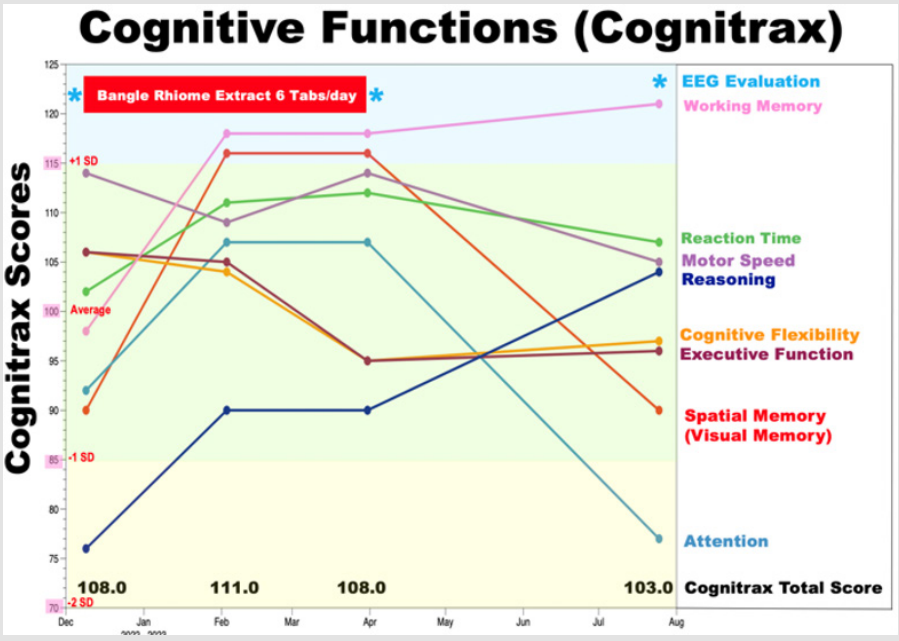


**Figure 5:** Cognitive functions before and after Bangle extract administration. Cognitive functions were evaluated by Cognitrax at four timepoints: December 9, 2022, February 3, 2023 (administration for 6 weeks), March 31, 2023 (administration for 12 weeks), and July 25, 2023 (follow-up after 4 months without Bangle extract). Cognitrax scores for working memory (magenta), reaction time (green), motor speed (plum), reasoning (dark blue), cognitive flexibility (orange), executive function (brown), spatial memory (visual memory, red), and attention (light blue) are shown chronologically. A Cognitrax score of 100 is the average score among the Japanese population of the same sex and age. Green indicates the zone of the average ± 1 SD, yellow indicates the zone from 1 SD to 2 SD less than the average, and blue indicates the zone + 1 SD over the average. The period of Bangle extract administration is shown in the upper part of the graph with a red box. Cognitrax total scores are shown at the bottom of the graph.

On March 31, 2023, 12 weeks after administration of BRE, a second cognitive function evaluation showed cognitive recovery for motor speed (109 -> 114) and maintenance of the cognitive enhancement for working memory (118 -> 118), spatial memory (116 -> 116), reaction time (111 -> 112), attention (107 -> 107), and reasoning (90 -> 90), while cognitive functions declined for cognitive flexibility (104 -> 95) and executive function (105 -> 95) (Figure 5). On July 25, 2023, after the washout period of 4 months without BRE, cognitive function evaluation showed further cognitive enhancement for working memory (118 -> 121) and reasoning (90 -> 104), while cognitive declines were observed for spatial memory (116 -> 90), attention (107 -> 77), motor speed (114 -> 105) and reaction time (112 ->107), with a decline in the Cognitrax Total Score (108.0 -> 103.0) (Figure 5). These data suggested that continuation of BRE administration may be necessary for the maintenance of improved cognitive functions such as attention, spatial memory, reaction time, and motor speed. We performed MRI on July 20, 2023, which showed the regeneration of damaged tissues in the medial part of the neck region in the left hippocampus (Figure 1C), red and blue arrows). Another endoscopic in silico view of the right hippocampus showed the fusion of fragmented hippocampal tissue (violet arrow) as well as the regeneration of fragmented hippocampal tissue (yellow arrow) (Figure 1D).

This is the first report to show that the medial parts of the hippocampal neck and head degrade into fragments during the degenerative process while the fragmented tissues fuse to the lateral part of the hippocampus (defragmentation), as shown in (Figure 1D) (violet arrow, fused; yellow arrow, defragmentation) in the regenerative process. Anatomically in the anterior part of the neck portion in the hippocampus (Figures 2A & 2C), the Dentate Gyrus (DG) is located in the medial part of the neck as well as inside of the neck (Figures 2A & 2C) red arrows). Since granular cells in the DG are more vulnerable than pyramidal cells in the CA1 and CA3 regions in the degenerative process [11] or multiple sclerosis [12], the loss of granular cells in the DG may result in fragmentation and loss of the medial part of the hippocampal neck, as shown in (Figures 2B & 2D). We re-evaluated the patients' EEG signals on March 24, 2023, which showed symmetrical P300 with higher voltages in both parietal leads after BRE administration (P3 and P4) (Figure 3A). The visual spatial memory test showed that the hyperexcitable EEG reaction observed before BRE administration was suppressed in both frontolateral leads (F7 and F8), while enhanced EEG reactions were observed in both frontopolar leads after BRE administration (FP1 and FP2) (Figure 3B), which was compatible with an improved spatial memory score with Cognitrax (Figure 5).

The attention test showed that the hyperexcitability observed before BRE administration was significantly suppressed after BRE administration (Figure 3C), suggesting that the regeneration of GABAergic interneurons suppresses the glutamatergic excitatory neurons evoked by the attention test as described previously [13,14]. The mental flexibility test also showed that the hyperexcitable reactions observed before BRE administration significantly suppressed the peak voltage of 4,500 $\mu V^2$ (Figure 3D) after BRE administration, which was compatible with an improved reasoning score with Cognitrax (Figure 5). Coherence analysis showed that the number of neural connections was more enhanced after BRE administration at the left temporal (T3 and T5), left central (C3), right frontolateral (F8), right temporal (T4 and T6), and right occipital (O2) leads (Figures 4B & 4D) than the neuronal connection before BRE administration (Figures 4A & 4C), suggesting that BRE facilitated neuronal connections and synapse formation in the cerebral cortex.

## Discussion

Bangle, Indonesian ginger (Zingibar Purpureum), is a tropical ginger widely distributed in Southeast Asia. A previous in vitro study using human foetal neural stem cells (hfNSCs) showed that Bangle Rhizome Extract (BRE) promoted neuronal differentiation from immature neurons and accelerated neurite outgrowth [7]. As shown in (Figure 6A), hfNSCs were treated with 10 ng/mL BRE and stained with anti-ßIII-tubulin antibody 7 days after induction of differentiation. The results showed that BRE induced the differentiation of hfNSCs in vitro compared to stem cells without BRE treatment. Furthermore, BRE induced the accumulation of ß-catenin in the nuclei of hfNSCs (Figure 6B) [7], suggesting that BRE activated the Wnt/ß-catenin pathway and induced gene expression for neurogenesis [7]. A previous study suggested that the Wnt/β-catenin signalling pathway plays an important role in neurogenesis and AD pathology [15,16]. As illustrated in (Figure 7), in the Wnt-off state (blue arrows), the GSK 3ß destruction complex (GSK3ß, Axin, Dvl, and other molecules) phosphorylates ß-catenin, which is subjected to the degradation pathway by the ubiquitin–proteasome system. GSK 3ß also phosphorylates tau at specific Ser and Thr residues that have been reported to be phosphorylated in Alzheimer's disease [17], suggesting that activation of canonical Wnt/ß-catenin signalling may delay the progression of AD pathology (Figure 7).

**DOI:** 10.26717/BJSTR.2023.52.008314

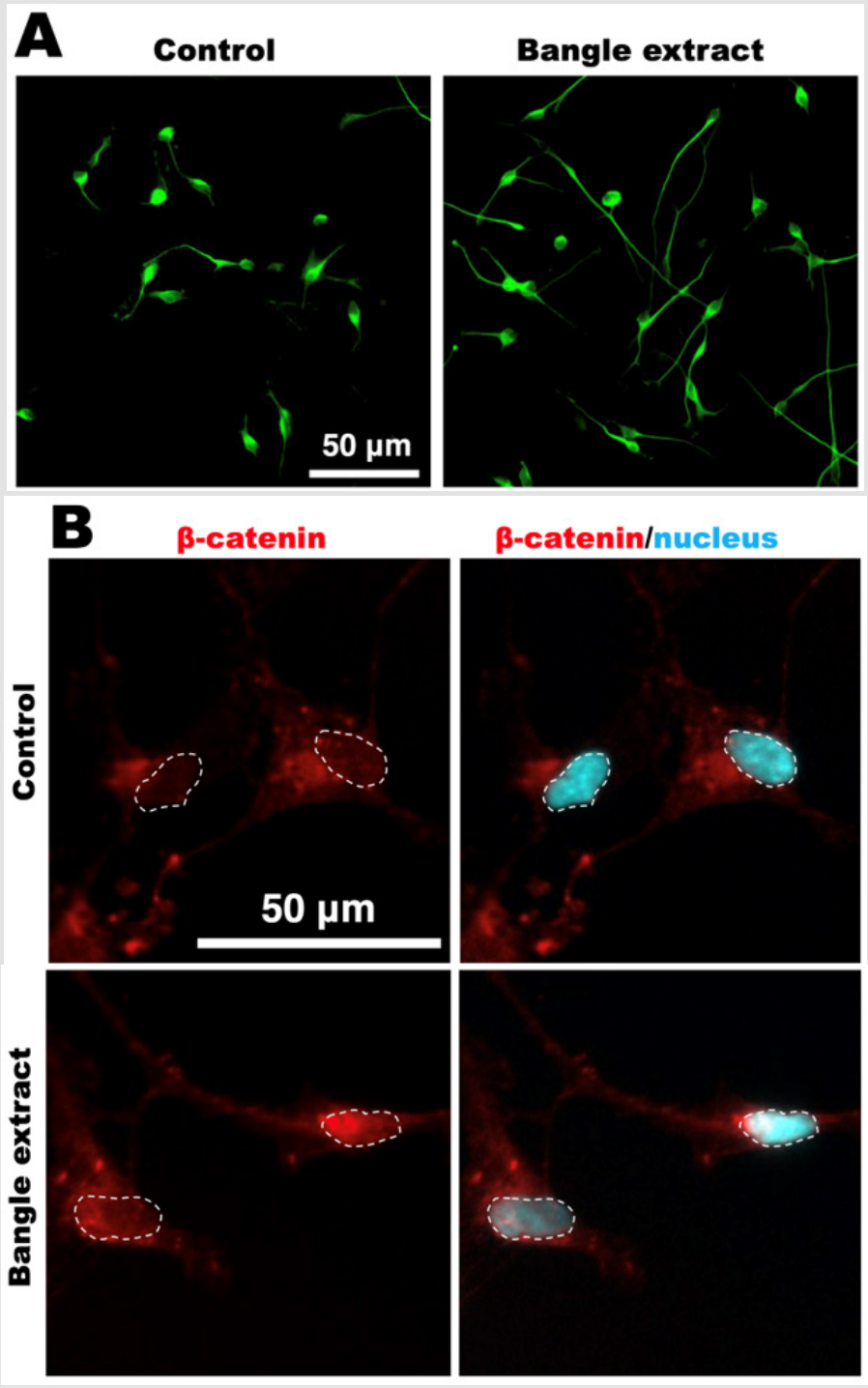


**Figure 6:** Bangle extract promotes neuronal differentiation of hfNSCs, neurite outgrowth in premature neurons, and Wnt signalling.
A. Cells treated with a series of concentrations of 10 ng/mL Bangle extract were stained with anti-βIII-tubulin antibody 7 days after induction of differentiation.
B. hfNSCs treated with 10 ng/ml Bangle extract for 2 days were stained with antibodies against β-catenin (red) and Hoechst (nucleus: cyan). The dotted line in each image represents the nucleus. Signals of β-catenin were increased in the nucleus of Bangle extract-treated hfNSCs compared to those of control cells. Scale bar: 50 μm.

**DOI:** 10.26717/BJSTR.2023.52.008314

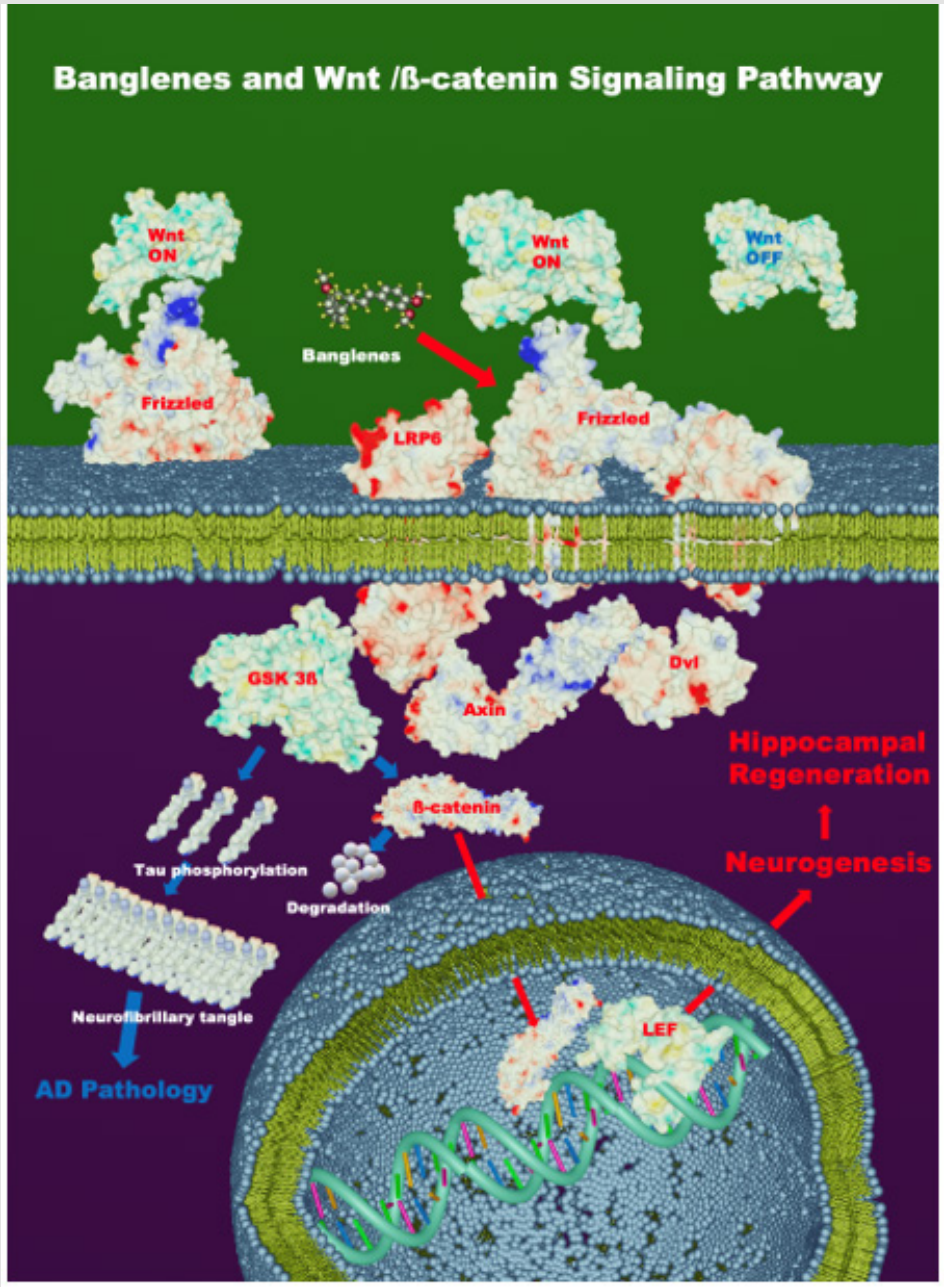


**Figure 7:** Banglenes and the Wnt/ß-catenin signalling pathway.
The Wnt/ß-catenin signalling pathway. In the Wnt-off state (blue arrows), the GSK 3ß destruction complex (GSK3ß, Axin, Dvl, and other molecules) phosphorylates ß-catenin in the degradation pathway by the ubiquitin-proteasome system and phosphorylates tau to form neurofibrillary tangles in AD pathology. In the Wnt-on state (red arrows), active Wnt ligands interact with the Frizzled receptors and the LRP5/6 coreceptor. Phosphorylation of LRP5/6 by GSK 3ß recruits Dvl and Axin to the receptor complex and inhibits the GSK 3ß destruction complex. This, in turn, inhibits ß-catenin phosphorylation and stabilizes ß-catenin in the cytoplasm. ß-catenin is then translocated into the nucleus and associates with the LEF complex, resulting in the upregulation of target gene expression for neurogenesis. Banglenes may activate Wnt/ß-catenin signalling pathway via Wnt ligand or Fizzled receptor. 3D structures of Wnt (PDB ID 4FOA), LRP6 (PDB ID 3S94), Frizzled (PDB ID 5CL1), Dvl (Dishevelled) (PDB ID 6ZBQ), Axin (PDB ID 1QZ7), GSK 3ß (PDB ID 2O5K), ß-catenin (PDB ID 2BCT), LEF (PDB ID 2LEF), tau (PDB ID 6NK4), and Banglenes (PubChem ID CID:53494256) were constructed by UCSF Chimaera-X Program (version 1.6.1). Plasma membrane, nuclear membrane, and DNA molecules with signalling molecules were assembled and rendered by Blender software (version 3.6.1).

In the Wnt-on state (red arrows), active Wnt ligands interact with the Frizzled receptors and the LRP5/6 coreceptor. Phosphorylation of LRP5/6 by GSK 3ß recruits Dvl and Axin to the receptor complex, which results in inhibition of the GSK 3ß destruction complex (Figure 7). In the Wnt-on state, the inhibition of ß-catenin phosphorylation stabilizes ß-catenin in the cytoplasm, which facilitates the translocation of ß-catenin into the nucleus and its association with the LEF transcriptional complex, resulting in the upregulation of the expression of genes related to neurogenesis, such as TBR2, DCX, DLX2, N-MYC, and EGFR, as previously described [7]. A previous study also suggested that BRE targets upstream molecules of the Wnt signalling pathway, such as ligands and receptors, including Frizzled (Figure 7), based on inhibitor experiments with XAV939, an inhibitor of the tankyrase (NKS) enzyme, or TWR-1-endo, an inhibitor that stabilizes the ß-catenin degradation complex [7]. It is thus speculated that BRE activates the Wnt/β-catenin signalling pathway to induce neurogenesis of neuronal stem cells in the hippocampus and cerebral cortex but also inhibits the progression of AD pathology (Figure 7). An MRI study showed the fusion of fragmented tissues in the medial part of the head and neck of the hippocampus (Figure 1D), suggesting that the neurogenesis of granule cells in the dentate gyrus of the hippocampus results in the morphological regeneration of the hippocampus with neuronal connections between granular cells in the DG and pyramidal cells in CA3 in the hippocampus (Figures 1 & 2).

Electrophysiological studies suggested that BRE induced the neurogenesis of GABAergic interneurons to suppress the hyperexcitability observed in the attention test and mental flexibility test (Figures 3C & 3D) and the neurogenesis of glutamatergic excitatory neurons, as shown in the visual spatial memory test (Figure 3B). The data suggested that BRE stimulated not only neuronal stem cells in the hippocampus but also neuronal stem cells residing in the cerebral cortex, as previously described [14,18-20].

## Conclusion

In the present case study, we applied Bangle Rhizome Extract (BRE) to a 53-year-old female patient with mild memory impairment for 6 weeks. Spatial memory, working memory, attention, and reaction time were improved after BRE administration in association with hippocampal neurogenesis. MRI showed the fusion of fragmented tissues in the hippocampus after BRE administration, which represents the morphological changes observed in the regenerative process of the hippocampus. This is the first clinical case report that BRE promotes neurogenesis and regeneration of the hippocampus associated with improved cognitive functions.

## Funding

This work was supported by a donation from HOSODA SHC Co., Ltd.

## Acknowledgement

The authors would like to thank Ms. Sayuri Sato, Ms. Masami Fukuda, Ms. Fernanda Diaz, and Dr Itzel Aguilar for the preparation of this manuscript.

## Ethical Approval of Studies and Informed Consent

Written informed consent was obtained from the patient.

## Conflict of Interest

The authors have no conflicts of interest.

## References

1. Sharifi Rad M, Varoni EM, Salehi B, Sharifi Rad J, Matthews KR, et al. (2017) Plants of the Genus Zingiber as a Source of Bioactive Phytochemicals: From Tradition to Pharmacy. Molecules 22(12): 2145.
2. Musdja MY (2021) Potential bangle (Zingiber montanum J.Konig) rhizome extract as a supplement to prevent and reduce symptoms of Covid-19. Saudi J Biol Sci 28: 2245-2253.
3. Kato E, Kubo M, Okamoto Y, Matsunaga Y, Kyo H, et al. Fukuyama Y (2018) Safety Assessment of Bangle (Zingiber purpureum Rosc.) Rhizome Extract: Acute and Chronic Studies in Rats and Clinical Studies in Human. ACS Omega 3: 15879-15889.
4. Kubo M, Gima M, Baba K, Nakai M, Harada K, et al. Fukuyama Y (2015) Novel neurotrophic phenylbutenoids from Indonesian ginger Bangle, Zingiber purpureum. Bioorg Med Chem Lett 25(7): 1586-1591.
5. Matsui N, Kido Y, Okada H, Kubo M, Nakai M, et al. Akagi M (2012) Phenylbutenoid dimers isolated from Zingiber purpureum exert neurotrophic effects on cultured neurons and enhance hippocampal neurogenesis in olfactory bulbectomized mice. Neurosci Lett 513(1): 72-77.
6. Nakai M, Iizuka M, Matsui N, Hosogi K, Imai A, et al. Miyamura M (2016) Bangle (Zingiber purpureum) Improves Spatial Learning, Reduces Deficits in Memory, and Promotes Neurogenesis in the Dentate Gyrus of Senescence-Accelerated Mouse P8. J Med Food 19(5): 435-441.
7. Hirano K, Kubo M, Fukuyama Y, Namihira M (2020) Indonesian Ginger (Bangle) Extract Promotes Neurogenesis of Human Neural Stem Cells through WNT Pathway Activation. Int J Mol Sci 21(13): 4772.
8. Gualtieri CT, Johnson LG (2006) Reliability and validity of a computerized neurocognitive test battery, CNS Vital Signs. Arch Clin Neuropsychol 21(7): 623-643.
9. Hirano K, Namihira M (2016) LSD1 Mediates Neuronal Differentiation of Human Fetal Neural Stem Cells by Controlling the Expression of a Novel Target Gene, HEYL. Stem Cells 34(7): 1872-1882.
10. Hirano K, Namihira M (2017) FAD influx enhances neuronal differentiation of human neural stem cells by facilitating nuclear localization of LSD1. FEBS Open Bio 7(12): 1932-1942.
11. Licht T, Kreisel T, Biala Y, Mohan S, Yaari Y, et al. Keshet E (2020) Age-Dependent Remarkable Regenerative Potential of the Dentate Gyrus Provided by Intrinsic Stem Cells. J Neurosci 40(5): 974-995.
12. Planche V, Koubiyr I, Romero JE, Manjon JV, Coupe P, et al. Tourdias T (2018) Regional hippocampal vulnerability in early multiple sclerosis: Dynamic pathological spreading from dentate gyrus to CA1. Hum Brain Mapp 39(4): 1814-1824.
13. Shirasawa T, Cobos LCA (2022) Cytokine-induced Neurogenesis for Alz-

heimer's Disease and Frontotemporal Dementia. Personalized Medicine Universe 11: 27-32.

14. Shirasawa T, Cobos LCA (2023) Cytokine-induced Neurogenesis Can Reverse Cognitive Decline in Alzheimer's Disease. Mathew Journal of Case Report 8(3): 1-7.
15. Arredondo SB, Valenzuela Bezanilla D, Mardones MD, Varela Nallar L (2020) Role of Wnt Signaling in Adult Hippocampal Neurogenesis in Health and Disease. Front Cell Dev Biol 8: 860.
16. Tapia Rojas C, Inestrosa NC (2018) Loss of canonical Wnt signaling is involved in the pathogenesis of Alzheimer's disease. Neural Regen Res 13(10): 1705-1710.
17. Kremer A, Louis JV, Jaworski T, Van Leuven F (2011) GSK3 and Alzheimer's Disease: Facts and Fiction. Front Mol Neurosci 4: 17.
18. Shirasawa T, Cobos LCA (2023) Cytokine-Induced Neurogenesis and Angiogenesis Reversed Cognitive Decline in a Vascular Dementia Patient with Hashimoto's Thyroiditis. ES J Case Rep 4: 1036.
19. Shirasawa T, Cobos LCA (2023) Cytokine-Induced Neurogenesis in Charcot-Marie-Tooth neuropathy with Connexin 32 Gene Mutation. Mathew Journal of Case Report 8(7): 1-9.
20. Mai JK, Majtanik M, Paxinos G (2016) Atlas of the Human Brain, (4th Edn.)., Academic Press.

**ISSN: 2574-1241**

DOI: 10.26717/BJSTR.2023.52.008314

**Takuji Shirasawa.** Biomed J Sci & Tech Res



**Submission Link**: https://biomedres.us/submit-manuscript.php